JOINT EUROPEAN TORUS

JET–P(92)53

The JET Team
(presented by P-H Rebut)

The JET Preliminary Tritium Experiment

The JET Preliminary Tritium Experiment

The JET Team*
(presented by P-H Rebut)

JET-Joint Undertaking, Culham Science Centre, OX14 3DB, Abingdon, UK

** See Annex*

Preprint of an Invited Talk given at the 1992 International Conference on Plasma Physics
(Innsbruck, Austria, 29th June -3rd July 1992)
and to be published in Plasma Physics and Controlled Fusion

THE JET PRELIMINARY TRITIUM EXPERIMENT

The JET Team* (presented by P-H Rebut)

JET Joint Undertaking. Abingdon, Oxon OX14 3EA, UK.

ABSTRACT

The first tokamak discharges with deuterium-tritium mixtures have been carried out in the Joint European Torus (JET). The main objectives were to produce more than 1MW of fusion power in a controlled way, to determine tritium retention in torus systems and to establish effective means of tritium removal. The experiments were undertaken within limits imposed by restrictions on vessel activation and tritium usage. Deuterium plasmas were heated by high power deuterium neutral beams from fourteen sources and fuelled by two neutral beam sources injecting tritium. In the best D-T discharge, the tritium concentration was about 11% at peak performance, when total neutron emission rate was 6.0×10^{17} s^{-1}, with 1.7MW of fusion power. The fusion amplification factor, Q_{DT} was 0.15. With optimum tritium concentration, this pulse would have produced a fusion power ≈5MW and nominal Q_{DT}=0.46. The same extrapolation for the best pure deuterium discharge gives about 11MW and a nominal Q_{DT}=1.14. Techniques for introducing, tracking, monitoring and recovering tritium were highly effective.

1 INTRODUCTION

The preliminary tritium experiment (JET Team, 1992) on the Joint European Torus (JET) had the following objectives:

(i) to produce in excess of 1MW of fusion power in a controlled way;
(ii) to validate transport codes and provide a basis for predicting accurately the performance of deuterium-tritium plasmas from measurements made in deuterium plasmas; to establish consistency of different experimental measurements; and to calibrate diagnostics;
(iii) to determine tritium retention in the torus walls and the neutral beam (NB) injection system; and to establish effective cleaning techniques for tritium removal;
(iv) to demonstrate technology related to tritium usage (tritium NB injection, cryopumping and tritium handling); and
(v) to establish safe procedures for handling tritium in compliance with the regulatory requirements.

At this stage in the JET programme, it was necessary to limit total neutron production to less than 1.5×10^{18} neutrons, so that resulting vessel activation would be compatible with divertor modification work presently in progress. In addition, the total tritium was restricted to about 0.2g (≈2000Ci) as the tritium processing plant is not scheduled to operate until 1993. Together, these limitations restricted the number of high performance discharges to two pulses.

2 TECHNICAL ASPECTS

2.1 Tritium introduction and collection systems

Neutral beam (NB) injection is effective in introducing tritium into the hot dense centre of the discharge, where the reactivity is highest and minimises the amount of tritium injected into the torus. Tritium gas was supplied from a uranium storage bed and buffer reservoir through a pressure regulator and needle valve and introduced into the neutralisers of two of the sixteen JET Positive Ion Neutral Injection sources, PINI's. The tritium gas introduction system was enclosed in a secondary containment system. About 6% of the tritium taken from the uranium storage bed was injected into the plasma as energetic neutrals: most of the tritium was collected on the cryopanels and ion beam dumps in the NB vacuum system and was subsequently recovered. This is the first time that an NB system has been used to inject energetic tritium neutrals at high power and long pulse duration into a fusion plasma and represents an important advance in this technology.

The two tritium PINIs operated at 78kV (deliberately operated below maximum performance to ensure high reliability) and injected 0.75MW each into the plasma. To conserve the limited amount of tritium, the change from

* See Appendix 1

deuterium to tritium was simulated in the NB Testbed using H and D gas. Consequently, prior to the D-T pulses, only two 1.5s tritium conditioning pulses were needed to change the beams from deuterium to tritium. The remaining fourteen PINI's were operated in deuterium: twelve at 135kV delivering 10.7MW and two at 75kV delivering 2.1MW. The tritium fuelling was ≈13% with two tritium PINI's. The programme of D-T experiments demonstrated reliable and efficient operation of the tritium NB injection and allowed experience to be gained both in handling, injecting and monitoring the usage of tritium and in recovering tritium from the torus and NB systems.

To collect and measure the injected tritium, the normal torus backing pump system was replaced by a cryogenic gas collection system, within a secondary containment system. During operation, the gas flow from the torus condensed on a tubular cryopump containing activated charcoal at liquid helium temperature. Subsequently, the condensed tritium, together with larger amounts of deuterium, was transferred to uranium storage beds for retrieval and separation. After the experiment, the NB cryopanels were warmed to release cryo-condensed gas which was collected in the cryogenic system in a similar way. The exhaust gases from both torus and NB systems were sampled for analysis and tritium assay and monitored before discharge to ensure compliance with statutory requirements. Using these techniques, the time dependent recovery of tritium from the torus and NB systems was assessed.

2.2 Recovery of tritium from the torus and NB systems

It was anticipated that full recovery of tritium from the large surface area of the torus would be relatively difficult and controlled clean-up experiments were performed to assess the effectiveness of various discharge techniques in removing tritium.

The total amount of tritium injected into the torus was 53(±4)Ci. In the 36 hours between the last tritium Pulse No. 26148 and the start of the clean-up experiments, ~15Ci were recovered on the tubular cryopump by pumping alone. The tritium concentration in successive clean-up discharges fell in accordance with a multi-reservoir development of the two reservoir model (Ehrenberg, 1987) established on the basis of data from hydrogen and deuterium discharges. During 25 pulses, the tritium released within 40 minutes of a pulse fell from 1Ci/pulse to 0.1Ci/pulse. Pulses which contacted different parts of the torus wall were used to remove tritium which, at least after the first few clean-up pulses, was distributed over the walls. A soak with D_2 gas after a series of pulses typically removed ≈0.1Ci. Nine days after the deuterium-tritium experiment, and after ≈100 pulses of various types, the tritium removal rate was ≈0.02Ci/pulse. Three weeks after the experiment, the removal rate was 3mCi/pulse and total tritium remaining in the torus walls was ≈15(±10)Ci, about one third of that injected.

Measurements on the tritium gas introduction system showed that 1000(±100)Ci were extracted from the uranium storage bed and introduced into the NB system for the two tritium pulses, of which 53(±4)Ci were estimated to have been injected into the torus. Following the experiment, the beams were injected into the beam calorimeters with the NB system valved off from the torus. Essentially all tritium on the beam dumps was desorbed in a small number of pulses, corresponding to the fluence of each PINI for about 100s. Monitoring the regeneration of the NB cryopumps through the gas collection system showed that, within the accuracy of measurements, essentially all tritium in the NB system was recovered. After a further regeneration and warming to room temperature, subsequent regenerations released only a few Ci from the NB system.

3 EXPERIMENTAL ARRANGEMENTS

3.1 Discharge details

The interior of the JET vacuum vessel consists of: a continuous top X-point target comprising plates clad with carbon fibre composite (CFC) tiles; a continuous bottom X-point target with beryllium tiles; a pair of outer wall toroidal belt limiters above and below the mid-plane (upper of beryllium and lower of carbon). All other plasma contacting surfaces, such as the inner wall, are of CFC , graphite or beryllium. Plasma contacting surfaces were extensively conditioned by a combination of glow discharge cleaning and tokamak discharge operation. Prior to the introduction of tritium, all plasma contacting components were coated with beryllium by periodically evaporating beryllium inside the vacuum vessel. A fresh layer was deposited about twelve hours before the experiment.

The highest neutron emission rates on JET have been obtained in hot-ion discharges (at low density with the ion temperature significantly higher than the electron temperature) in the H-mode regime. A single-null X-point discharge, diverted onto the upper carbon target, with reversed toroidal magnetic field, was selected for these experiments. In this configuration (Fig. 1), ions drift away from the target towards the plasma. This leads to more equal power loading between the inner and outer branches of the X-point. This configuration allows consistently higher energy input and longer duration of the high performance phase before a "carbon bloom" occurs.

3.2 Diagnostics

Over thirty diagnostics were in operation for this experiment. These included magnetic measurements (used to determine the equilibrium configuration and the plasma diamagnetic energy), electron cyclotron emission (for the

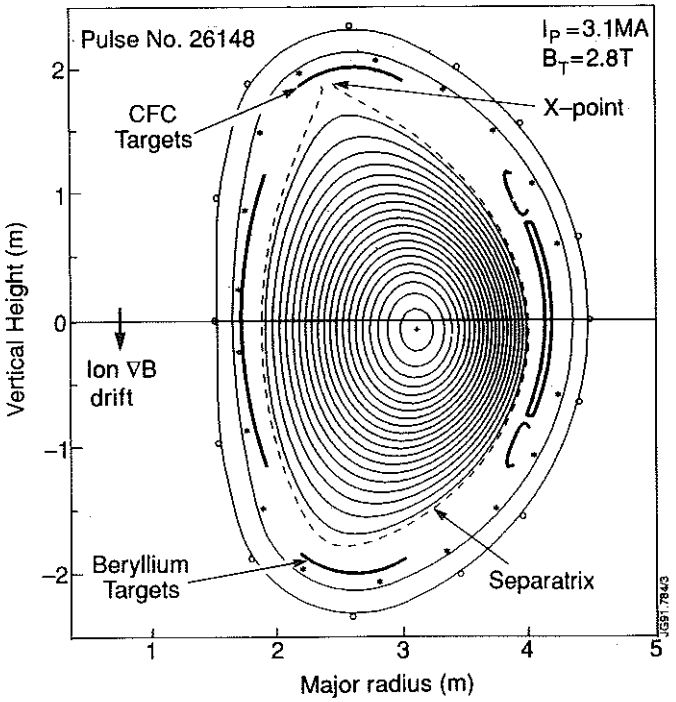

FIG. 1. The magnetic configuration with magnetic axis at R_{mag}=3.15m, horizontal minor radius, a=1.0m, elongation, κ=1.6 and safety factors, q_ψ=3.8 and q_{cyl}=2.8. Shown are the separatrix, X-point, ion ∇B drift and CFC and beryllium targets.

electron temperature, T_e), an infra-red interferometer (for the electron density, n_e), LIDAR Thomson scattering (for T_e and n_e), active charge exchange recombination spectroscopy (for the ion temperature, T_i and impurity concentrations) and visible bremsstrahlung (for the effective ionic charge, Z_{eff}).

Time-dependent neutron emission rates were measured with silicon surface barrier diodes (which exploited the high threshold energy of (n,p) and (n,α) nuclear reactions in silicon to record 14MeV neutrons) and using ^{235}U and ^{238}U fission chambers (which were not capable of discriminating 2.5MeV and 14MeV neutrons). The accuracy of the total neutron yield was ±7%. The neutron spectrum was measured with a liquid scintillator spectrometer. A flat pulse height distribution is obtained up to the maximum energy corresponding to the complete transfer of neutron energy to the recoiling proton. Neutron emission profile data can be obtained from 19 similar spectrometers arranged in two cameras with orthogonal views of a vertical section of plasma. 2.5MeV and 14MeV neutrons are distinguished, except when high fluxes of 14MeV neutrons inhibit measurement of low fluxes of 2.5MeV neutrons.

4 EXPERIMENTAL RESULTS

Results from two discharges in the series of experiments are described. The first is a high-performance pure deuterium discharges (Pulse No. 26087), and the second is a D-T discharge with a 100% mixture of tritium introduced into two PINI's (Pulse No. 26148, one of two similar discharges). In these cases, the plasma current started to increase at time, t=0, was maintained at a "flat-top" <3MA from 5s to 15s and then decreased towards zero, which was reached at ~25s.

4.1 Pure deuterium discharge

Fig. 2 shows the time development of certain characteristic parameters during the current "flat-top" of Pulse No. 26087, including central temperatures, average density, Z_{eff}, plasma diamagnetic energy and total neutron emission rates. The plasma target for NB injection is formed by allowing the density to fall during the transition from a limiter to an X-point configuration. The result is a moderately peaked density profile. At 12s the NB power increases to ≈15MW, which leads, after 0.3s, to the transition to the H-mode phase. During the subsequent 1s, sawteeth are stabilised and the centrally peaked NB heating produces peaked temperature profiles. Ion and electron temperatures rise continuously throughout this phase, reaching 18.6keV and 10.5keV, respectively. The plasma diamagnetic energy reaches 11.6MJ, corresponding to a ratio of plasma to magnetic pressure of 2.2%. The plasma profiles are shown in Fig. 3(a). The high performance phase is terminated at a time (13.4s) characterized by a rise in edge emission from CIII and D_α (the "carbon bloom"), followed by a sawtooth collapse of the central temperatures. Nevertheless, the H-mode persists until the high power NB injection is switched off at 14s. The time development of these discharges is typical of hot-ion H-modes with characteristically long sawtooth-free periods of up to 1.5s.

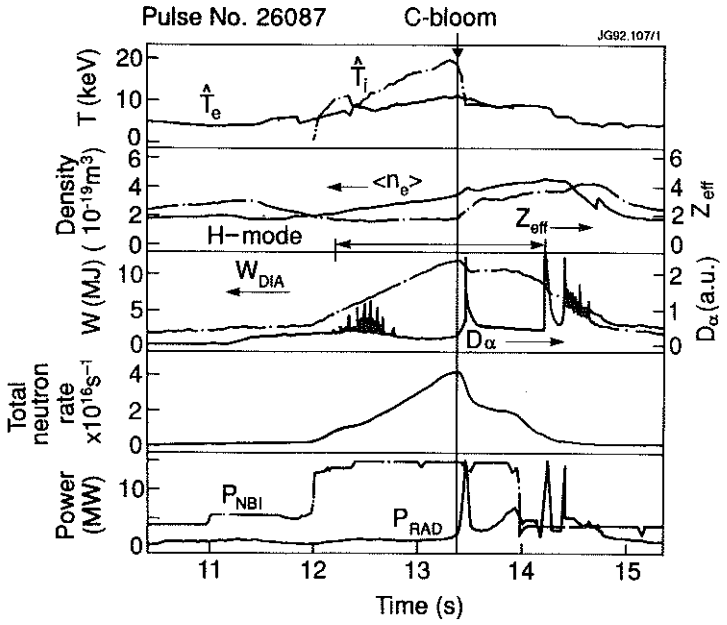

FIG. 2. Time development of central electron and ion temperatures, volume-averaged electron density, line-averaged $\overline{Z}_{eff}$, plasma diamagnetic energy, D_α emission, total neutron rate, and NB and radiated powers for Pulse No. 26087.

The TRANSP code (Goldston et al, 1981) was used to check the internal consistency of measured data and to estimate the fraction of neutrons produced by thermal-thermal, beam-thermal and beam-beam reactions on the basis of measured profiles of n_e, T_e and T_i and Z_{eff} (with an assumed flat profile). In particular, measurement and simulation were compared for diamagnetic and MHD energies, loop voltage and, most importantly, the neutron emission rates. As shown in Fig.4, there is good agreement between measured and simulated emission rates for 2.5MeV neutrons. The simulation also showed that ≈60% of the neutrons were produced by thermal-thermal reactions, while the remainder were mostly by beam-thermal reactions, with a small fraction by beam-beam reactions.

4.2 Discharge with 100% tritium in two PINI's

To minimise activation levels and tritium usage, only two pulses were attempted. Both were similar and each produced fusion power in excess of 1.5MW. The NB power profile was chosen to give effective fuelling, as predicted by the TRANSP code and confirmed by test discharges with 1% tritium in one PINI. These discharges

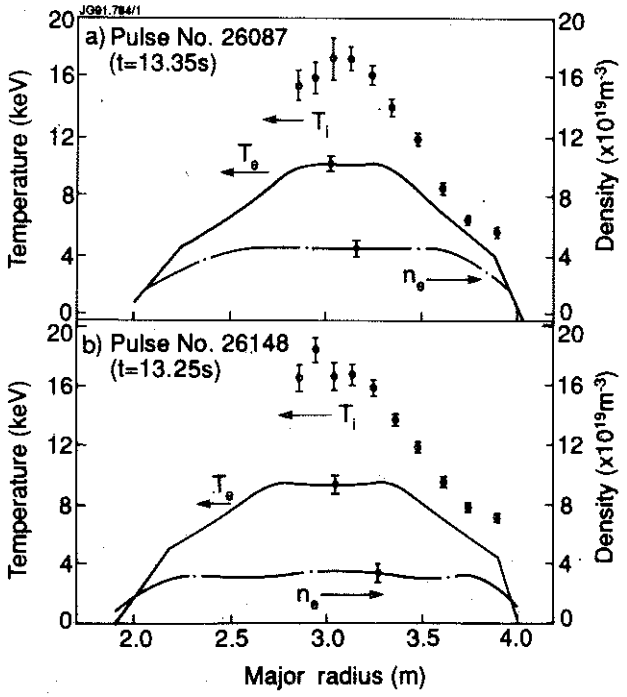

FIG. 3. Radial profiles of electron and ion temperatures and electron density for (a) Pulse No. 26087 and (b) Pulse No. 26148.

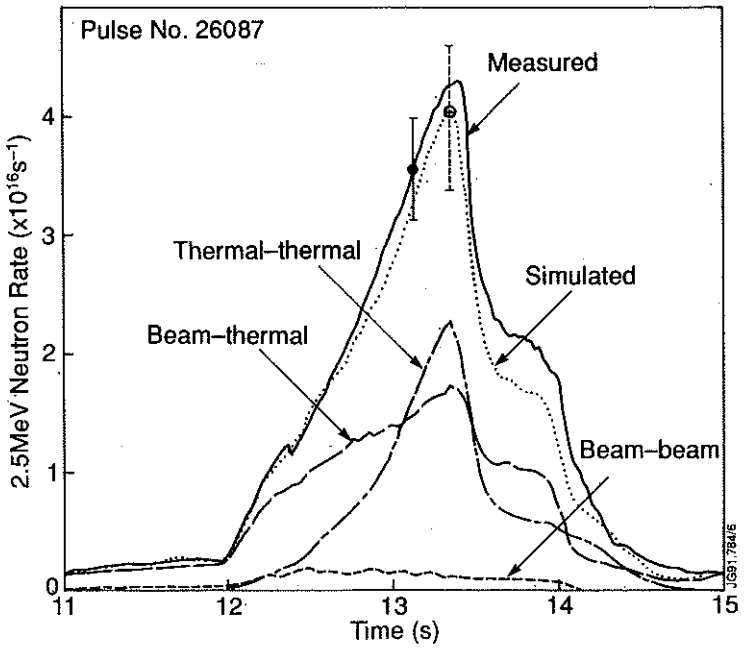

FIG. 4: The measured and simulated neutron rates for 2.5MeV neutrons for Pulse No. 26087.

were also heated by up to four deuterium PINI's, before and after high power heating. This suppressed MHD instabilities at early times and secured a disruption-free decay of the plasma current at late times.

Fig.5 shows the time development of characteristic parameters for Pulse No. 26148 and all increase throughout the H-mode phase of the discharge, starting at 12.4s and ending with a "carbon bloom" at 13.3s. The plasma profiles are shown in Fig.3(b). The proton recoil pulse height spectrum for Pulse No. 26147 (Fig.6) shows clearly the presence of 14MeV neutrons. The total emission is about forty times that obtained for 2.5MeV neutrons in a similar deuterium discharge (Pulse No. 26143). The 14MeV neutrons, which interact with carbon nuclei in the scintillator, also give rise to the high emission observed at a few MeV.

Data consistency is again demonstrated by the good agreement obtained between the measured and simulated emission of, predominantly, 14MeV neutrons (see Fig.7). Again, the simulations showed that ≈50% of the neutrons were produced by thermal-thermal reactions while the remainder were mostly by beam-thermal reactions with only a small fraction by beam-beam reactions. The peak total neutron emission rate was 6.0x10^{17} neutrons/s in an high

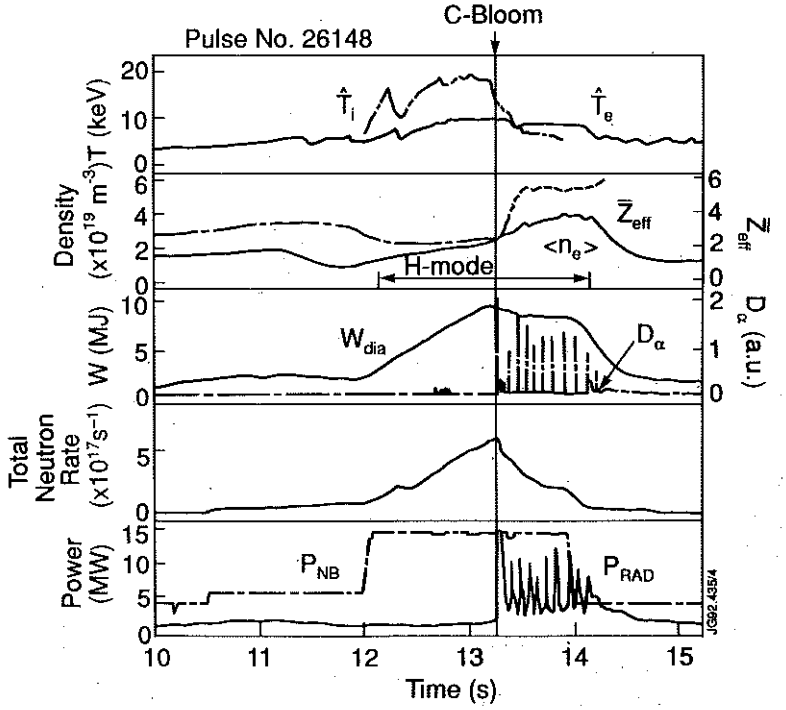

FIG. 5. Time development of the central electron and ion temperatures, volume-averaged electron density, line-averaged $\bar{Z}_{eff}$, plasma diamagnetic energy, D_α emission, total neutron rate, and the NB and radiated powers for Pulse No. 26148. After the "carbon bloom", the Z_{eff} measurement (- - -) is affected by black body radiation emanating from the targets.

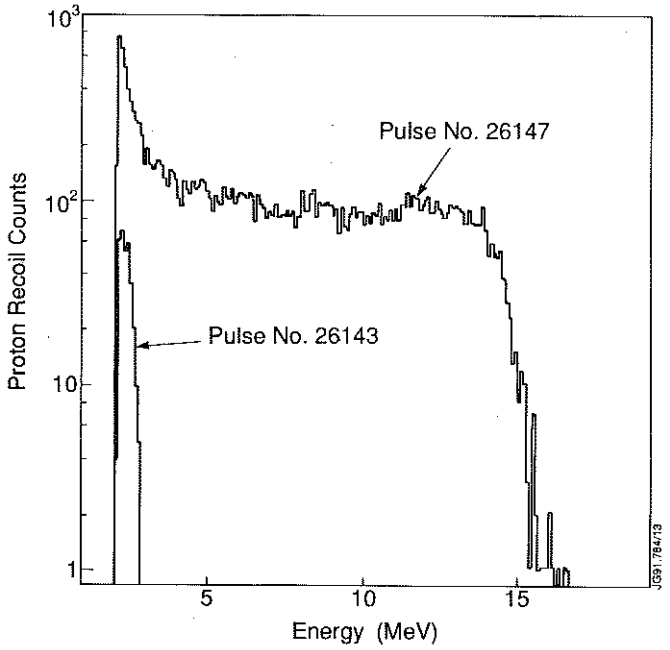

FIG. 6. Proton pulse height spectrum for D-T Pulse No. 26147 (mainly 14MeV neutrons) and deuterium Pulse No. 26143 (2.5MeV neutrons only).

power phase lasting about 2s. The integrated total neutron yield was 7.2×10^{17} neutrons with an accuracy of ±7%. The total fusion releases (α-particles and neutrons) were 1.7MW of peak power and 2MJ of energy.

The simulation also showed that the level of α-particle heating was too low, in comparison with the NB power, to have a discernible effect on electron temperature. Furthermore, the α-particle pressure and concentration were probably too low for the stimulation of collective effects. While these effects cannot be excluded entirely, the characteristics of the MHD activity in the tritium discharges were very similar to those of pure deuterium discharges such as Pulse No. 26087.

5 EXTRAPOLATION TO FULL PERFORMANCE D-T DISCHARGES

The fusion amplification factor, Q_{DT}, is defined in terms of the separate contributions from thermal-thermal, Q_{tt}, beam-thermal, Q_{bt}, and beam-beam, Q_{bb}, reactions:

$$Q_{DT} = Q_{tt} + Q_{bt} + Q_{bb}$$

where $Q_{tt} = P_{tt} / (P_{loss} - 0.2P_{tt})$, $Q_{bt} = P_{bt} / (P_b - P_{st})$, and $Q_{bb} = P_{bb} / (P_b - P_{st})$

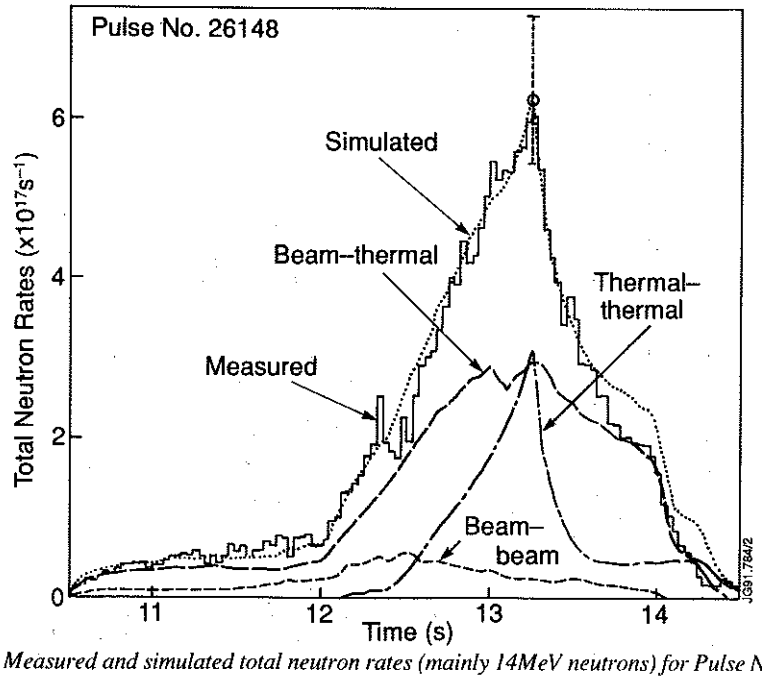

FIG. 7. Measured and simulated total neutron rates (mainly 14MeV neutrons) for Pulse No. 26148.

P_{tt}, P_{bt} and P_{bb} are the total fusion powers, respectively, from thermal-thermal, beam-thermal and beam-beam reactions, $P_{loss} = P_b + P_\Omega - P_{st} - dW/dt + P_{\alpha x}$ is the total power lost from the plasma (including radiation and charge-exchange) and P_b, P_Ω, P_{st}, dW/dt and $P_{\alpha x}$ are, respectively, the NB input power, the ohmic input power, the power lost by NB "shine-through", the rate of change of plasma diamagnetic energy andthe actual experimentally achieved α-power. With this definition, it is easy to evaluate Q_{DT} for an actual plasma using the separation into thermal-thermal, beam-thermal and beam-beam powers given by the TRANSP code. At peak neutron emission in Pulse No. 26148, Q_{DT} determined in this way is 0.15.

To estimate Q_{DT} which would be obtained for a similar discharge but with a more optimum D-Tmixture, a nominal Q_{DT} is defined as the value that would be obtained if the hydrogen isotope content of the plasma were replaced instantaneously by the more optimum mixture with a tritium concentration, $c = \langle n_T \rangle / (\langle n_D \rangle + \langle n_T \rangle)$. At the times of peak neutron emission, and with c=0.6, nominal Q_{DT} is 0.46 in deuterium-tritium Pulse No. 26148, and 1.14 in deuterium Pulse No. 26087.

This nominal Q_{DT} is similar to that which would have been obtained experimentally if eight of the sixteen PINI's (instead of two in Pulse No. 26148 and none in Pulse No. 26087) had been used to inject tritium into a 50:50 deuterium-tritium target plasma. TRANSP simulations of these two pulses, with the actual plasma conditions and NB power and acceleration voltages used in the experiment, then gives Q_{DT}=0.44 for Pulse No. 26148 and 1.07 for Pulse No. 26087 (in each case the value of c is determined by NB injection and is about 0.5). The total fusion power (neutrons and α-particles) and the fraction coming from thermal-thermal reactions for the two pulses would be 4.6MW(43%) and 9.6MW(57%), respectively.

In the future, for the main D-T experiments planned for 1996, there will be 12.5MW of tritium NB injection at a principal energy of 160kV and 8MW of deuterium NB injection at a principal energy of 140kV. The higher power and better beam penetration should give higher values of Q_{DT}. Up to 20MW of ICRH, should be available either alone or in combination with NB heating, in which case the total fusion power should also increase. The pumped divertor is expected to control impurities and give a cleaner plasma, which should further increase Q_{DT}.

6 SIMULATION OF THESE DISCHARGES

Experimental observations support a model for anomalous transport based on a single phenomenon and MHD limits. The Critical Electron Temperature Gradient model of anomalous heat and particle transport is one such model. Specifically, above a critical threshold, $(\nabla T_e)_{cr}$, in the electron temperature gradient, the transport is anomalous and greater than the underlying neoclassical transport. The electrons are primarily responsible for the anomalous transport, but ion heat and particle transport are also anomalous. The general expressions for the anomalous conductive heat fluxes have been specified (Rebut et al, 1992). The model exhibits the following experimental features: consistency with physics constraints, global scaling laws and statistical analysis; a limitation in the electron temperature; no intrinsic degradation of ion confinement with ion heating power; no dependence of confinement on mass; and similar behaviour of particle heat and transport. The model, which has no free parameters, reproduces plasma profiles for a wide variety of discharges in OH, L- and H- regimes in various tokamaks.

Pulses Nos: 26087 and 26148 were simulated using this model in the plasma interior and, at the L to H transition, imposing a narrow, edge region with neoclassical transport. The simulated temperature profiles at different times during the hot-ion H-mode phase of the discharges show good agreement with the measurements (Figs.8(a) and 9(a)). Over much of the discharge the calculated effective electron and ion thermal diffusivities (Figs.8(b) and 9(b)) increase with radius and decrease with time. χ_i is about 50% larger than χ_e and both show some structure in the discharge centre where the error is large due to uncertainties in the precise geometry, heating profile and q-profile.

7 DISCHARGE TERMINATION AND VARIABILITY

These high performance discharges were limited by a "carbon bloom". The time of occurrence affected the maximum neutron emission rates (shown in Fig. 10) and, for a given magnetic configuration, was principally dependent on the level and duration of heating, characterised by the total energy, E_C, conducted to the X-point targets (Stork, 1991):

$$E_c = \int_{t_{X-point}}^{t_{bloom}} \left(P_{tot} - P_{rad} - \frac{dW}{dt} \right) dt$$

where P_{tot} is total input power, P_{rad} the radiated power and dW/dt the rate of change of energy. For the configuration, power and duration in these experiments, the "carbon bloom" occurred when E_C was typically 11±3MJ. In some cases, this occurred "naturally", presumably due to progressive rise of target temperature. In other cases, when the conducted energy was in this range, the "carbon bloom" could be triggered by a MHD event, such as a giant ELM. or a sawtooth collapse which coupled to an ELM. The occurrence of these events appears to depend upon the precise time evolution of plasma density and additional heating and showed some variability in these experiments.

In comparison with other similar discharges in deuterium, the high performance phase of both deuterium-tritium Pulse Nos. 26147 and 26148 terminated as the result of a somewhat earlier sawtooth collapse, coupled

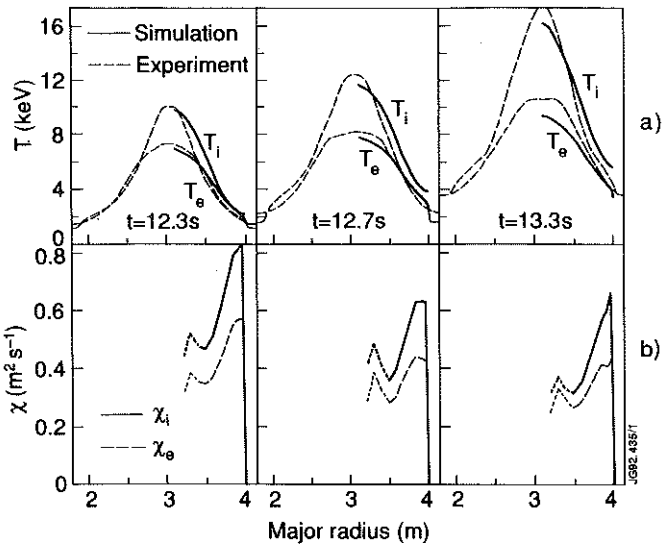

FIG.8: Simulation of Pulse No:26087 with Critical Electron Temperature Gradient model.

to an ELM and leading to the "carbon bloom" (1.3s after the start of full NB power, see Fig. 10 for Pulse No. 26148). Detailed analysis of the collapse shows that the inversion radius of such sawteeth was no larger than for normal sawteeth. However, a strong coupling between central and edge modes was observed and might have played a role in triggering the ELM, which occurred within 100μs of the sawtooth collapse.

8 SUMMARY AND CONCLUSIONS

In JET, high performance deuterium discharges with $Q_{DD}>2x10^{-3}$ and nominal $Q_{DT}>0.5$ are obtained routinely and reliably. The best JET deuterium pulse gave $Q_{DD}\approx5x10^{-3}$ and a nominal $Q_{DT}=1.14$, so that the total fusion power (neutrons and α-particles) would exceed the total losses in the equivalent deuterium-tritium discharge in these transient conditions.

For the first time, experiments on high fusion performance tokamak plasmas have been performed using a deuterium-tritium fuel mixture. Techniques used for introducing, tracking, monitoring and recovering tritium were highly effective. Essentially all of the tritium introduced into the NB system has been recovered and, so far, about two thirds that introduced into the torus. These levels are sufficiently low for the JET experimental programme in deuterium to continue normally. The wall tiles were removed at the start of the present shutdown, and post-mortem analysis should provide important data for the choice of wall materials for a Next Step device.

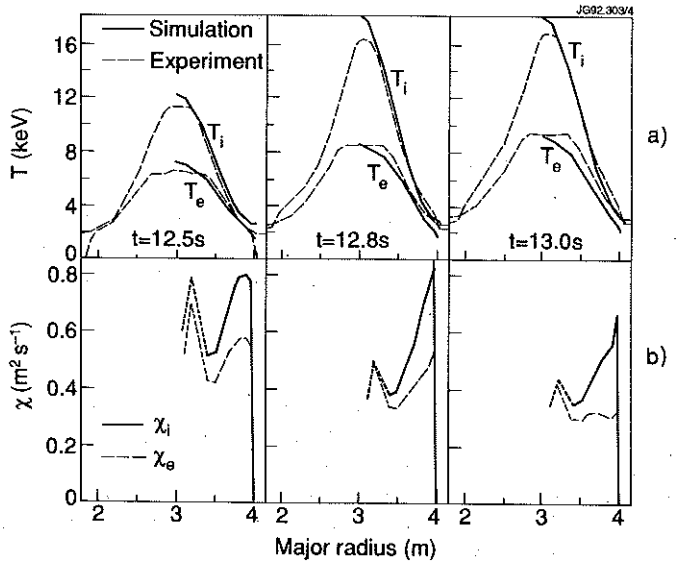

FIG.9: Simulation of Pulse No:26148 with Critical Electron Temperature Gradient model.

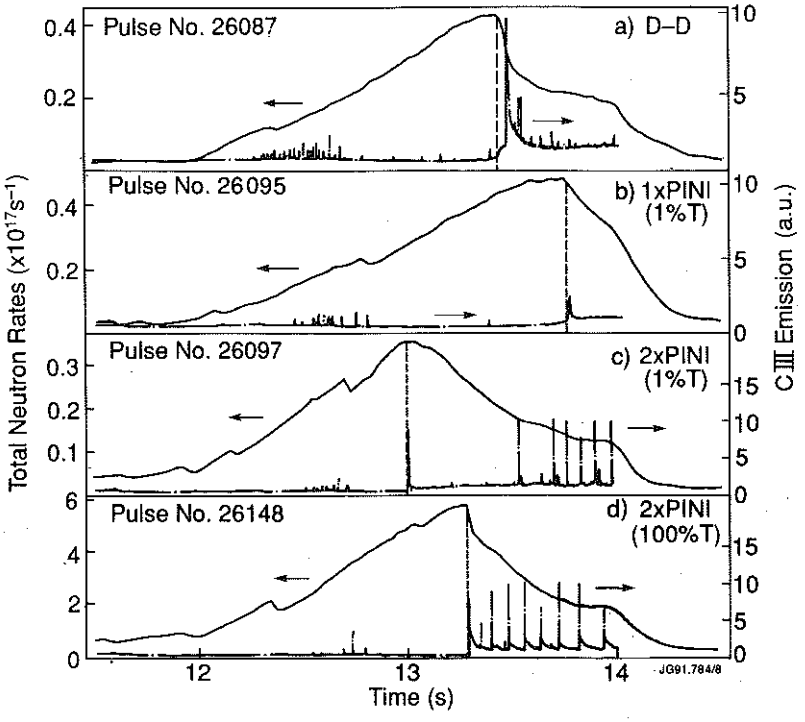

FIG. 10. Variation in time of termination of the high performance phase of a number of similar discharges shown by the fall in neutron emission rate. The dashed vertical lines show the time of the "carbon bloom" as characterized by increased emission of CIII light from the plasma edge. In (a) and (b), the bloom occurs "naturally"; in (c) it is triggered by an ELM; and in (d) by a sawtooth collapse coupled to an ELM.

Tritium NB was injected into a deuterium plasma, heated by deuterium neutral beams. The tritium concentration was ≈11% at the time of peak performance when the total neutron emission rate was 6.0×10^{17} neutrons/s. The integrated total neutron yield over the high power phase, which lasted about 2s, was 7.2×10^{17} neutrons, with an accuracy of ±7%. The total fusion releases were 1.7MW at peak power and 2MJ of energy. The amount of tritium injected and the number of discharges with tritium were deliberately restricted for operational convenience.

The consistency of the experimental data was established with simulations using the TRANSP code which showed, in particular, that thermal-thermal and beam-thermal reactions contributed about equally to the total neutron emission. The good agreement obtained between measurement and simulation gave confidence in the accuracy of extrapolations from existing discharges. Assuming a tritium concentration, $c = \langle n_T \rangle / (\langle n_D \rangle + \langle n_T \rangle) = 0.6$ (chosen near the optimum for fusion power output), the deuterium-tritium Pulse No. 26148 would have produced a fusion power of ≈5MW and a nominal $Q_{DT} \approx 0.46$. The same extrapolation for the pure deuterium Pulse No. 26087 would have given ≈11MW and a nominal $Q_{DT} = 1.14$. Use of the more optimum NB system intended for JET in 1996, together with control of the impurity influx as envisaged with the JET pumped divertor, should yield higher values of Q_{DT}.

The temperature profile for both the high performance deuterium discharge and the tritium discharge are well simulated by the critical electron temperature gradient model for energy and particle transport. The effective electron and ion thermal diffusivities are low everywhere ($<1 m^2 s^{-1}$) increasing with time and plasma radius. With this model, we begin to have the predictive capability needed to define the parameters and operating conditions of a reactor. However, the transient nature of the type of H-mode discharge used for the deuterium-tritium experiment emphasises the need to control the "carbon bloom" and to develop a viable mode of operation for a reactor. Controlling the plasma exhaust and the ingress of impurities released at the divertor plates will be the major theme of the JET Programme to 1995. These data, together with those on tritium retention and further preliminary tritium experiments, should allow the planning of an effective campaign of D-T experiments in 1996. These should also permit accurate extrapolations to a Next Step device, that is, to one designed to operate routinely at a temperature sustained by its own fusion power.

REFERENCES

Ehrenberg, J. (1987), *J. Nucl. Mater.*, **145-147** 551.
Goldston, R.J., McClune, D.C., Towner, H.H., et al., (1981), *J. Comput. Phys.* **43** 61.
JET Team, (1992), *Nuclear Fusion* **32(2)** 187.
Rebut, P-H., Watkins, M.L., Gambier, D.J., and Boucher.D, (1992), *Phys. Fluids (B)*, **3(8)** 2209
Stork, D, et al, (1991), Proc. 18th Eur. Conf. (Berlin), Vol.15C, Part 1 p.357

Appendix I

THE JET TEAM

JET Joint Undertaking, Abingdon, Oxon, OX14 3EA, U.K.

J.M. Adams[1], B. Alper, H. Altmann, A. Andersen[14], P. Andrew, S.Ali-Arshad, W. Bailey, B. Balet, P. Barabaschi, Y. Baranov, P. Barker, R. Barnsley[2], M. Baronian, D.V. Bartlett, A.C. Bell, G. Benali, P. Bertoldi, E. Bertolini, V. Bhatnagar, A.J. Bickley, D. Bond, T. Bonicelli, S.J. Booth, G. Bosia, M. Botman, D. Boucher, P. Boucquey, M. Brandon, P. Breger, H. Brelen, W.J. Brewerton, H. Brinkschulte, T. Brown, M. Brusati, T. Budd, M. Bures, P. Burton, T. Businaro, P. Butcher, H. Buttgereit, C. Caldwell-Nichols, D.J. Campbell, D. Campling, P. Card, G. Celentano, C.D. Challis, A.V.Chankin[23], A. Cherubini, D. Chiron, J. Christiansen, P. Chuilon, R. Claesen, S. Clement, E. Clipsham, J.P. Coad, I.H. Coffey[24], A. Colton, M. Comiskey[4], S. Conroy, M. Cooke, S. Cooper, J.G. Cordey, W. Core, G. Corrigan, S. Corti, A.E. Costley, G. Cottrell, M. Cox[7], P. Crawley, O. Da Costa, N. Davies, S.J. Davies[7], H. de Blank, H. de Esch, L. de Kock, E. Deksnis, N. Deliyanakus, G.B. Denne-Hinnov, G. Deschamps, W.J. Dickson[19], K.J. Dietz, A. Dines, S.L. Dmitrenko, M. Dmitrieva[25], J. Dobbing, N. Dolgetta, S.E. Dorling, P.G. Doyle, D.F. Düchs, H. Duquenoy, A. Edwards, J. Ehrenberg, A. Ekedahl, T. Elevant[11], S.K. Erents[7], L.G. Eriksson, H. Fajemirokun[12], H. Falter, J. Freiling[15], C. Froger, P. Froissard, K. Fullard, M. Gadeberg, A. Galetsas, L. Galbiati, D. Gambier, M. Garribba, P. Gaze, R. Giannella, A. Gibson, R.D. Gill, A. Girard, A. Gondhalekar, D. Goodall[7], C. Gormezano, N.A. Gottardi, C. Gowers, B.J. Green, R. Haange, A. Haigh, C.J. Hancock, P.J. Harbour, N.C. Hawkes[7], N.P. Hawkes[1], P. Haynes[7], J.L. Hemmerich, T. Hender[7], J. Hoekzema, L. Horton, J. How, P.J. Howarth[5], M. Huart, T.P. Hughes[4], M. Huguet, F. Hurd, K. Ida[18], B. Ingram, M. Irving, J. Jacquinot, H. Jaeckel, J.F. Jaeger, G. Janeschitz, Z. Jankowicz[22], O.N. Jarvis, F. Jensen, E.M. Jones, L.P.D.F. Jones, T.T.C. Jones, J-F. Junger, F. Junique, A. Kaye, B.E. Keen, M. Keilhacker, W. Kerner, N.J. Kidd, R. Konig, A. Konstantellos, P. Kupschus, R. Lässer, J.R. Last, B. Laundy, L. Lauro-Taroni, K. Lawson[7], M. Lennholm, J.Lingertat[13], R.N. Litunovski, A. Loarte, R. Lobel, P. Lomas, M. Loughlin, C. Lowry, A.C. Maas[15], B. Macklin, C.F. Maggi[16], G. Magyar, V. Marchese, F. Marcus, J. Mart, D. Martin, E. Martin, R. Martin-Solis[8], P. Massmann, G. Matthews, H. McBryan, G. McCracken[7], P. Meriguet, P. Miele, S.F. Mills, P. Millward, E. Minardi[16], R. Mohanti[17], P.L. Mondino, A. Montvai[3], P. Morgan, H. Morsi, G. Murphy, F. Nave[27], S. Neudatchin[23], G. Newbert, M. Newman, P. Nielsen, P. Noll, W. Obert, D. O'Brien, J. O'Rourke, R. Ostrom, M. Ottaviani, S. Papastergiou, D. Pasini, B. Patel, A. Peacock, N. Peacock[7], R.J.M. Pearce, D. Pearson[12], J.F. Peng[26], R. Pepe de Silva, G. Perinic, C. Perry, M.A. Pick, J. Plancoulaine, J-P. Poffé, R. Pohlchen, F. Porcelli, L. Porte[19], R. Prentice, S. Puppin, S. Putvinskii[23], G. Radford[9], T. Raimondi, M.C. Ramos de Andrade, M. Rapisarda[29], P-H. Rebut, R. Reichle, S. Richards, E. Righi, F. Rimini, A. Rolfe, R.T. Ross, L. Rossi, R. Russ, H.C. Sack, G. Sadler, G. Saibene, J.L. Salanave, G. Sanazzaro, A. Santagiustina, R. Sartori, C. Sborchia, P. Schild, M. Schmid, G. Schmidt[6], H. Schroepf, B. Schunke, S.M. Scott, A. Sibley, R. Simonini, A.C.C. Sips, P. Smeulders, R. Smith, M. Stamp, P. Stangeby[20], D.F. Start, C.A. Steed, D. Stork, P.E. Stott, P. Stubberfield, D. Summers, H. Summers[19], L. Svensson, J.A. Tagle[21], A. Tanga, A. Taroni, C. Terella, A. Tesini, P.R. Thomas, E. Thompson, K. Thomsen, P. Trevalion, B. Tubbing, F. Tibone, H. van der Beken, G. Vlases, M. von Hellermann, T. Wade, C. Walker, D. Ward, M.L. Watkins, M.J. Watson, S. Weber[10], J. Wesson, T.J. Wijnands, J. Wilks, D. Wilson, T. Winkel, R. Wolf, D. Wong, C. Woodward, M. Wykes, I.D. Young, L. Zannelli, A. Zolfaghari[28], G. Zullo, W. Zwingmann.

PERMANENT ADDRESSES

1. UKAEA, Harwell, Didcot, Oxon, UK.
2. University of Leicester, Leicester, UK.
3. Central Research Institute for Physics, Budapest, Hungary.
4. University of Essex, Colchester, UK.
5. University of Birmingham, Birmingham, UK.
6. Princeton Plasma Physics Laboratory, New Jersey, USA.
7. UKAEA Culham Laboratory, Abingdon, Oxon, UK.
8. Universidad Complutense de Madrid, Spain.
9. Institute of Mathematics, University of Oxford, UK.
10. Freien Universität, Berlin, F.R.G.
11. Royal Institute of Technology, Stockholm, Sweden.
12. Imperial College, University of London, UK.
13. Max Planck Institut für Plasmaphysik, Garching, FRG.
14. Risø National Laboratory, Denmark.
15. FOM Instituut voor Plasmafysica, Nieuwegein, The Netherlands.
16. Dipartimento di Fisica, University of Milan, Milano, Italy.
17. North Carolina State University, Raleigh, NC, USA
18. National Institute for Fusion Science, Nagoya, Japan.
19. University of Strathclyde, 107 Rottenrow, Glasgow, UK.
20. Institute for Aerospace Studies, University of Toronto, Ontario, Canada.
21. CIEMAT, Madrid, Spain.
22. Institute for Nuclear Studies, Otwock-Swierk, Poland.
23. Kurchatov Institute of Atomic Energy, Moscow, USSR
24. Queens University, Belfast, UK.
25. Keldysh Institute of Applied Mathematics, Moscow, USSR.
26. Institute of Plasma Physics, Academica Sinica, Hefei, P. R. China.
27. LNETI, Savacem, Portugal.
28. Plasma Fusion Center, M.I.T., Boston, USA.
29. ENEA, Frascati, Italy.

At 1st July, 1992